

STIMULATED BREMSSTRAHLUNG IN LINEARLY POLARIZED LASER FIELDS OF RELATIVISTIC INTENSITIES

A.G. Markossian

E-mail: amarkos@ysu.am

Centre of Strong Fields Physics, Yerevan State University, 1 A. Manoogian, Yerevan 0025, Armenia

Received July 10, 2009

The stimulated bremsstrahlung (SB) of electrons in the field of superstrong laser radiation of linear polarization, in the scope of relativistic quantum theory is investigated (in the Born approximation for the scattering potential). The multiphoton cross sections of high-intensity laser radiation absorption by electrons due to SB have been obtained by numerical simulations.

PACS numbers: 42.50.Hz, 34.80.Rm, 31.15.-p, 34.50.Rk

Apart from general physical interests as an important induced electromagnetic (e.m.) process, the stimulated bremsstrahlung (SB) of electrons on the plasma ions/atoms, or at the scattering on arbitrary electrostatic potentials in the presence of strong e.m. radiation field, is one of the dominant mechanisms of e.m. radiation absorption in plasma, specifically for its laser heating at high temperatures. The existence of current ultrapower laser sources rather exceeding already the threshold value of relativistic intensities 10^{18} W/cm² in optical domain [1], has increased the interest to the mentioned problem at the interaction of such superstrong radiation fields with the underdense plasma. Hence, it is of certain interest to study the dynamics of SB process in the laser fields of high relativistic intensities.

The nonrelativistic analytical treatment of the elementary process of SB in the Born approximation has been developed in the work [2], which then was extended for a relativistic domain [3]. Relativistic effects in the SB corresponding to the first Born approximation with the comparison to a spinless and a nonrelativistic treatment for the circularly polarized e.m. wave have been investigated in the papers [4, 5]. The low-frequency (LF) approximation for SB in the relativistic case was carried out in the work [6]. The investigations of the relativistic dynamics of SB, as well as the nonlinear absorption of an electron beam due to SB process in the LF approximation at the arbitrary intensities of an external e.m. radiation field, particularly at the asymptotically large values of the dimensionless relativistic invariant parameter of wave intensity $\xi = eE/mc\omega \gg 1$ (E is the electric field strength, and ω -frequency of a wave; m and e are the electron mass and charge, respectively; c is the light speed in vacuum) were done in the papers [7, 8]. In the work [9] so-called eikonal approximation was developed in the relativistic quantum scattering theory for a spinor Dirac particle on an arbitrary electrostatic field and then it was

developed for the SB process - generalized eikonal approximation (GEA) [10]. This GEA wave function is applicable in both quantum and quasiclassical limits, i.e., connects the particle wave functions of the Born and ordinary eikonal approximations. The relativistic cross-sections of SB and for above threshold ionization (ATI) of atoms rates in the scope of the GEA approximation with straightforward analytical treatments for circular polarization of e.m. wave in the limit of Born approximation were done in the papers [11, 12]. Note that the ATI of atoms by intense laser pulses has enabled cold plasmas to be created [13]. It is clear that the final temperature of such plasmas depends on the heating process during the laser pulse action. Connected with this problem the nonlinear absorption of superpower laser radiation of arbitrary intensities (at asymptotically large values of ξ) by relativistic Maxwellian plasma due to the inverse SB has been investigated in the work [14].

For a wide range of laser parameters SB process can be considered without collective plasma effects. It is well known that the kinematics of an electron in the field of a strong e.m. wave essentially depends on the polarization of the wave. Thus, since the wave intensity for a circular polarization $\xi^2 = \text{const}$, then the longitudinal velocity of the electron in the wave: $V_{||} = \text{const}$ too, meanwhile in the wave of a linear polarization $V_{||}$ oscillates with the wave harmonics $n\omega$, corresponding to unharmonic oscillatory motion of the electron. The latter leads to more complicated behavior of the dynamics of electron induced interaction with additional third body at the linear polarization of a stimulating strong wave. For example, in contrast to circular polarization [12], in case of a linearly polarized e.m. wave to obtain ultimate results for relativistic ATI rates, taking into account the photoelectron SB, is impossible analytically [15]. The analogous situation takes place for relativistic cross-sections of SB in the strong linearly polarized radiation field, the consideration of which is the matter of the present paper. On the other hand, many important laser assisted processes/nonlinear phenomena just occur at the linear polarization of the stimulating field (when conservation laws of a process require a certain symmetry of the photon field). Thus, the high harmonic generation (HHG) process on the atoms takes place only in the linearly polarized laser fields [16].

In this paper the investigation of relativistic cross-sections of SB of electrons at the scattering on a screening Coulomb potential in the presence of a linearly polarized strong laser radiation of relativistic intensities will be completed with the numerical treatment of the issue.

We use the analytic formulas for differential multiphoton cross-sections of SB [11] for an electron scattering on a screening Coulomb potential

$$\varphi(r) = -\frac{Z_a e}{r} e^{-\lambda r},$$

in the field of linearly polarized e.m. wave of high intensity. Here $1/\chi$ is the radius of screening, Z_a is the charge number of a nucleus. The linearly polarized quasimonochromatic e.m. wave will be described by the vector potential:

$$\vec{A} = \vec{e}A_0 \cos(\omega t - \vec{k}\vec{r}), \quad (1)$$

with the slowly varying amplitude A_0 and \vec{e} is the unit polarization vector ($\vec{e} \perp \vec{k}$). From the general formula for partial differential cross-sections (in the differential solid angle $d\Omega$) [11], in case of a linearly polarized wave we have the following expression:

$$\begin{aligned} \frac{d\sigma^{(n)}}{d\Omega} = & \frac{Z_a^2 e^4 m^2 |\Pi'|}{|\Pi| |\vec{q}_n^2 + \chi^2|^2} \left\{ J_n^2(u, v) \left[\varepsilon^2 - \vec{q}_n^2 - \beta^2 \left(\frac{1}{2} + \frac{n}{4v} \right) \right] + \right. \\ & + \left[J_{n-1}(u, v) + J_{n+1}(u, v) \right]^2 \left[\omega^2 \alpha'^2 + \frac{\beta^2}{4} \right] + \\ & \left. + J_n(u, v) \left[J_{n-1}(u, v) + J_{n+1}(u, v) \right] \left[\frac{u\beta^2}{8v} - 2\omega\varepsilon\alpha' \right] \right\}. \end{aligned} \quad (2)$$

Here

$$J_n(u, v) = \sum_{k=-\infty}^{\infty} J_{n-2k}(u) J_k(v) \quad (3)$$

is the generalized Bessel function, $\Pi = (\Pi_0, \vec{\Pi})$ is the average four-kinetic momentum or "quasimomentum" of the electron in the plane e.m. wave. The latter is defined via the free electron four-momentum $p = (\varepsilon_0, \vec{p})$ and four-wave vector $k = (\omega, \vec{k})$ as

$$\Pi = p + kZ, \quad (4)$$

where $Z = e^2 \bar{A}_0^2 / 4kp$ is the relative parameter of the wave intensity (\bar{A}_0 is the averaged value of the vector-potential amplitude A_0). The arguments of the generalized Bessel function and the interaction parameters are defined as follows:

$$u = e\bar{A}_0 \left(\frac{\vec{e}\vec{p}'}{kp'} - \frac{\vec{e}\vec{p}}{kp} \right), \quad v = \frac{Z - Z'}{2}, \quad (5)$$

$$\beta^2 = \frac{e^2 \bar{A}_0^2}{(kp)(kp')} \left[\omega^2 \vec{q}_n^2 - (\vec{k}\vec{q}_n)^2 \right], \quad (6)$$

$$\varepsilon = 2\Pi_0 + \frac{n\omega Z}{v}, \quad \alpha' = e\bar{A}_0 \frac{\vec{e}\vec{p}}{kp} + \frac{uZ}{2v}, \quad (7)$$

Here $\vec{q}_n = \Pi_n \hat{r} - \vec{\Pi} - n\vec{k}$ and $\Pi_n = |\vec{\Pi}'| = \sqrt{\vec{\Pi}^2 + n\omega(2\Pi_0 + n\omega)}$ is the final quasimomentum of the particle corresponding to n -photon absorption ($n > 0$) and emission ($n < 0$) processes. The formula (2) is obtained in the Born approximation for the electron scattering. In the Coulomb field

the condition of the Born approximation holds if initial and final mean velocities of the electron obey the condition $V, V' \gg Z_a / 137$.

Comparing the nonrelativistic cross-section [2] with relativistic one (2) it is easy to see that besides the additional terms, which come from spin-orbital and spin-laser interactions ($\approx \vec{q}_n^2$) as well as the effect of intensity $\approx \xi^2$, the relativistic contribution is conditioned by arguments of the generalized Bessel function $J_n(u, v)$ (3). Because of sensitivity of the Bessel function to relationship of its argument and index, the most probable number of emitted or absorbed photons will be defined by the condition $|n| \approx |u| \approx |v|$. By this reason the contribution of relativistic effects on the scattering process becomes essential already for $\xi \approx 0.1$ [4], consequently, the dipole approximation is violated for nonrelativistic parameters of interaction.

As was mentioned above, the treatment of the nonlinear processes in case of the linear polarization of e.m. wave is very complicated and we need the numerical simulations. For all numerical calculations it is assumed Ti-sapphire laser ($\omega = 0.058 a.u.$). The radius of screening is taken to be $\chi^{-1} = 4 a.u.$ and charge number of nucleus $Z_a = 1$. In contrast to a circular polarization of an e.m. wave, at the linear polarization there is not the azimuthal symmetry, but since the main contribution in the cross-section is made by the scattering in the plane formed by the vectors \vec{e} and \vec{k} , we present the results of the numerical simulations for the azimuthal angle $\varphi = 0$.

In Fig.1(a) the envelopes of partial differential cross-sections as a function of the number of absorbed/emitted photons are shown for the deflection angle ($\theta = \angle \vec{\Pi} \vec{\Pi}'$) $\theta = 0.6$ mrad, for an intensity of Ti-sapphire laser 0.8×10^{18} W/cm², that corresponds to the relativistic parameter of intensity $\xi = 0.6$. The electron moves \vec{k} in the laser propagation direction \vec{k} with initial kinetic energy $\varepsilon_k = 2U_p$ ($U_p = e^2 E^2 / 4m\omega^2$ is the ponderomotive potential, defined as the mean energy acquired by an electron (initially in rest) in the oscillating e.m. wave).

In Fig. 1(b) and 1(c) the laser field intensities and deflection angles are taken to be 2.2×10^{18} W/cm² ($\xi = 1$), $\theta = 60$ μ rad and 4.9×10^{18} W/cm² ($\xi = 1.5$), $\theta = 6$ μ rad, respectively. Note that the intensity parameter can be expressed by the intensity I and wavelength λ_L of the e.m. wave as follows:

$$\xi = 8.5 \times 10^{-6} \lambda_L [cm] \sqrt{I [W / cm^2]}. \quad (8)$$

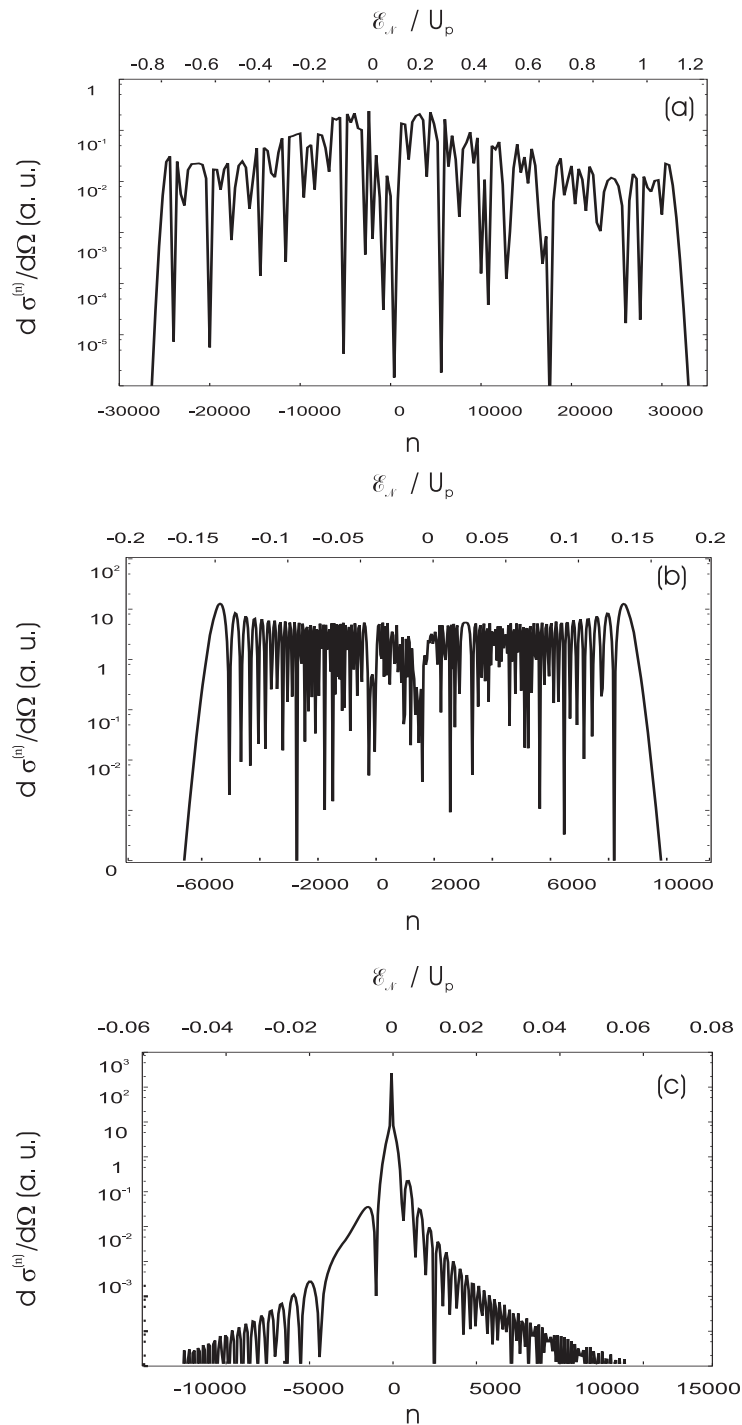


Fig. 1. The envelopes of partial differential cross-sections $d\sigma^{(n)}/d\Omega$ in atomic units as a function of the number of emitted or absorbed photons, for the linear polarization of Ti-sapphire laser ($\omega=0.058$ a.u.), in logarithmic scale. The laser field intensities are taken to be (a) 0.8×10^{18} W/cm² ($\xi=0.6$) for the deflection angle $\theta=0.6$ mrad, (b) 2.2×10^{18} W/cm² ($\xi=1$) for the deflection angle $\theta=60$ μ rad, and (c) 4.9×10^{18} W/cm² ($\xi=1.5$) for the deflection angle $\theta=6$ μ rad. The electron moves in the laser propagation direction \vec{k} with the initial energy $2U_p$.

In Fig. 2 the envelopes of partial differential cross-sections $d\sigma^{(n)}/d\Omega$ as a function of the number of emitted or absorbed photons are shown for various laser parameters and deflection angles. The dashed curve corresponds to initial electron momentum antiparallel to the laser propagation direction \vec{k} , and solid curve gives the nonrelativistic result.

The comparison of the SB cross-sections in case of linear polarization of e.m. wave from Figs. 1 and 2 shows that when the initial momentum of an electron is parallel to the laser propagation direction \vec{k} , the cutoff positions of partial differential cross-sections exceed by orders of magnitude the cutoff with antiparallel momentum.

To clear up the dependence of the SB process on the laser field polarization in Figs. 3 and 4 the envelopes of partial differential cross-sections for circular polarization of e.m. wave are shown. Figures 3 and 4 are the counterparts of Figs. 1 and 2, respectively. To emphasize the differences, the relativistic parameter of intensity and the deflection angle are taken the same. As is seen from these figures, SB process for large intensities of the laser field essentially depends on the laser field polarization. In particular, the absorption and emission cutoff positions and the peak values are essentially different.

The energy change of a particle is characterized by the absorption/emission (AE) cross-section. Partial AE differential cross-sections are defined as:

$$\frac{d\sigma_{AE}^{(n)}}{d\Omega} = n \left(\frac{d\sigma^{(n)}}{d\Omega} - \frac{d\sigma^{(-n)}}{d\Omega} \right). \quad (9)$$

In Figure 5 the envelopes of partial AE differential cross-sections for linear polarization of e.m. wave are shown for the large deflection angles at the moderate relativistic intensity of Ti-sapphire laser $\xi = 0.2$. In this case for an electron initial energy we have taken moderate value $\varepsilon_k = 2.7$ keV. The dotted and dashed curves correspond to initial electron momentum parallel and antiparallel to the laser propagation direction \vec{k} , respectively. The solid curve gives the nonrelativistic result. As seen from Fig. 5, the differences between these cases are evident already at $\xi \ll 1$; in particular, the magnitudes of the peaks are essentially different.

To illustrate the angular distribution of relativistic multiphoton cross-sections of the SB process at the linearly polarized strong e.m. wave field ($\xi \geq 1$) and to compare it with the case of circular polarization of the wave, in Fig. 6 we display the partial differential cross-section as a function of the deflection angle θ at the fixed number of photons (n_p). To make parallels with ATI process we will take the number of photons which corresponds to the most hot photoelectrons in the ATI process of atom: $n_p = 2U_p / \omega$ for the linearly polarized e.m. wave and $n_p = 4U_p / \omega$ for the circularly polarized one. With the increase in e.m. wave intensity and, consequently the relativism of electrons, the angular distribution of multiphoton SB becomes anisotropic with respect to polarization vector of e.m. wave.

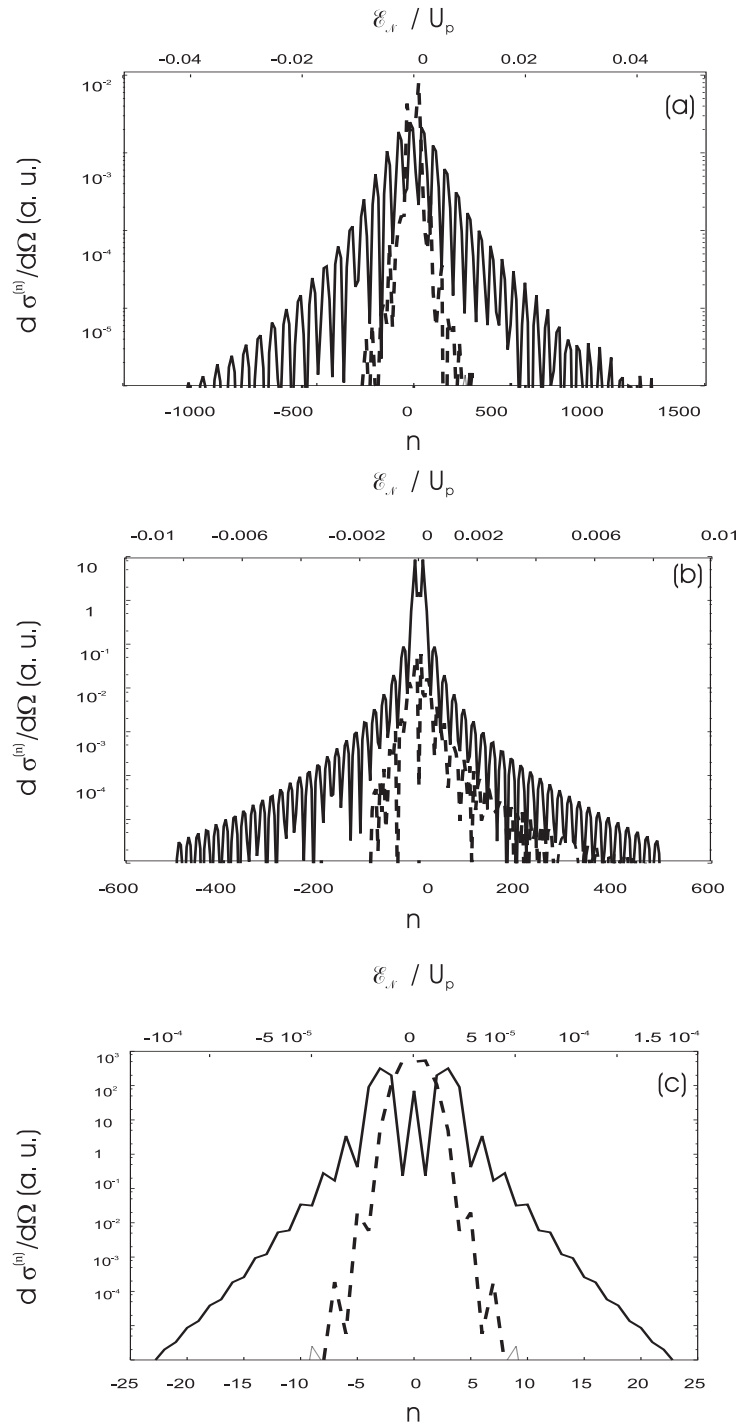


Fig. 2. The envelopes of partial differential cross-sections $d\sigma^{(n)}/d\Omega$ as a function of the number of emitted or absorbed photons, for the linear polarization of Ti-sapphire laser, in logarithmic scale. The dashed line corresponds to initial electron momentum antiparallel to the laser propagation direction and the solid line gives the nonrelativistic result. The case (a) corresponds to $\xi=0.6$ for the deflection angle $\theta=0.6$ mrad, (b) $\xi=1$ for the deflection angle $\theta=60$ μ rad, and (c) $\xi=1.5$ for the deflection angle $\theta=6$ μ rad. The initial energy of the electron is taken to be $2U_p$.

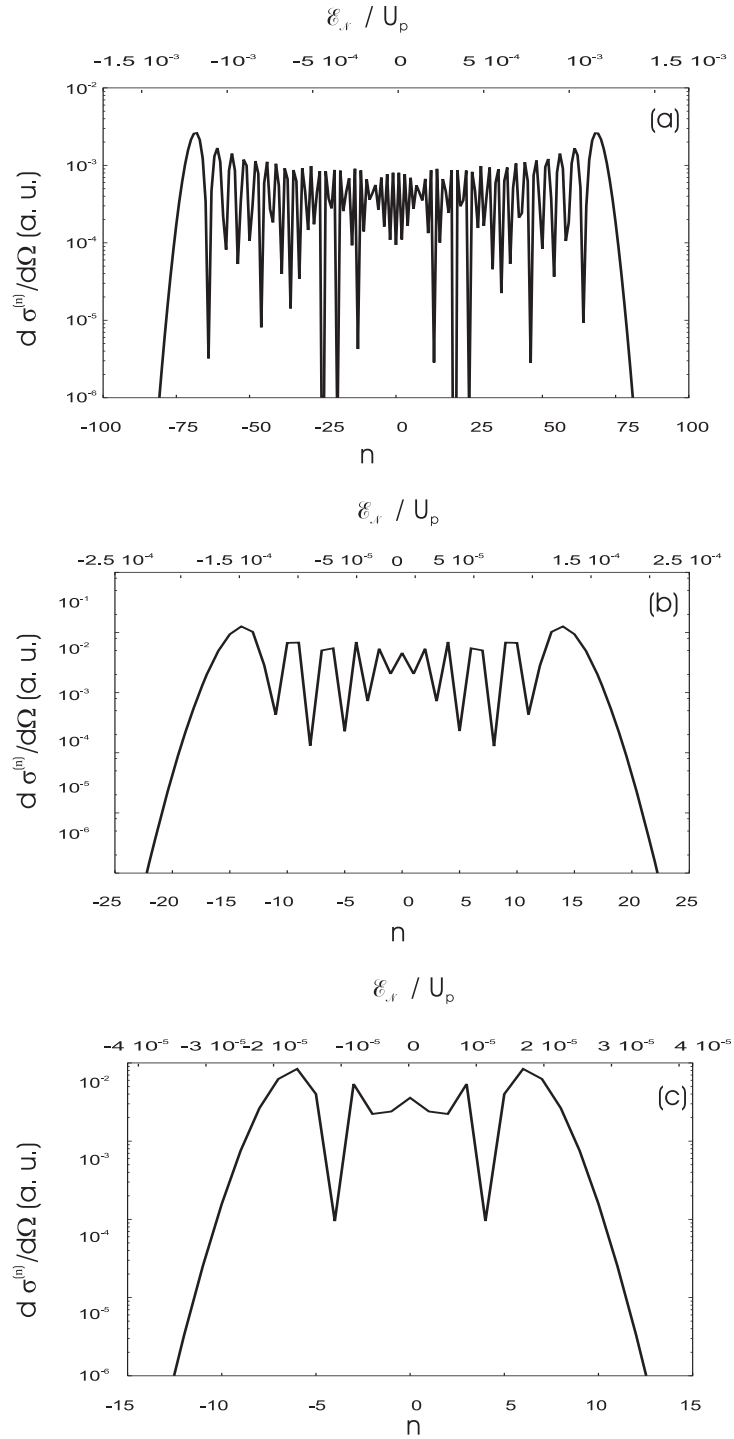


Fig. 3. The envelopes of partial absorption or emission differential cross-sections are shown for the circularly polarized Ti-sapphire laser, in logarithmic scale. The electron moves in the laser propagation direction \vec{k} with the initial energy $4U_p$. (a) $\xi=0.6$ for the deflection angle $\theta=0.6$ mrad, (b) $\xi=1$ for the deflection angle $\theta=60$ μ rad, and (c) $\xi=1.5$ for the deflection angle $\theta=6$ μ rad.

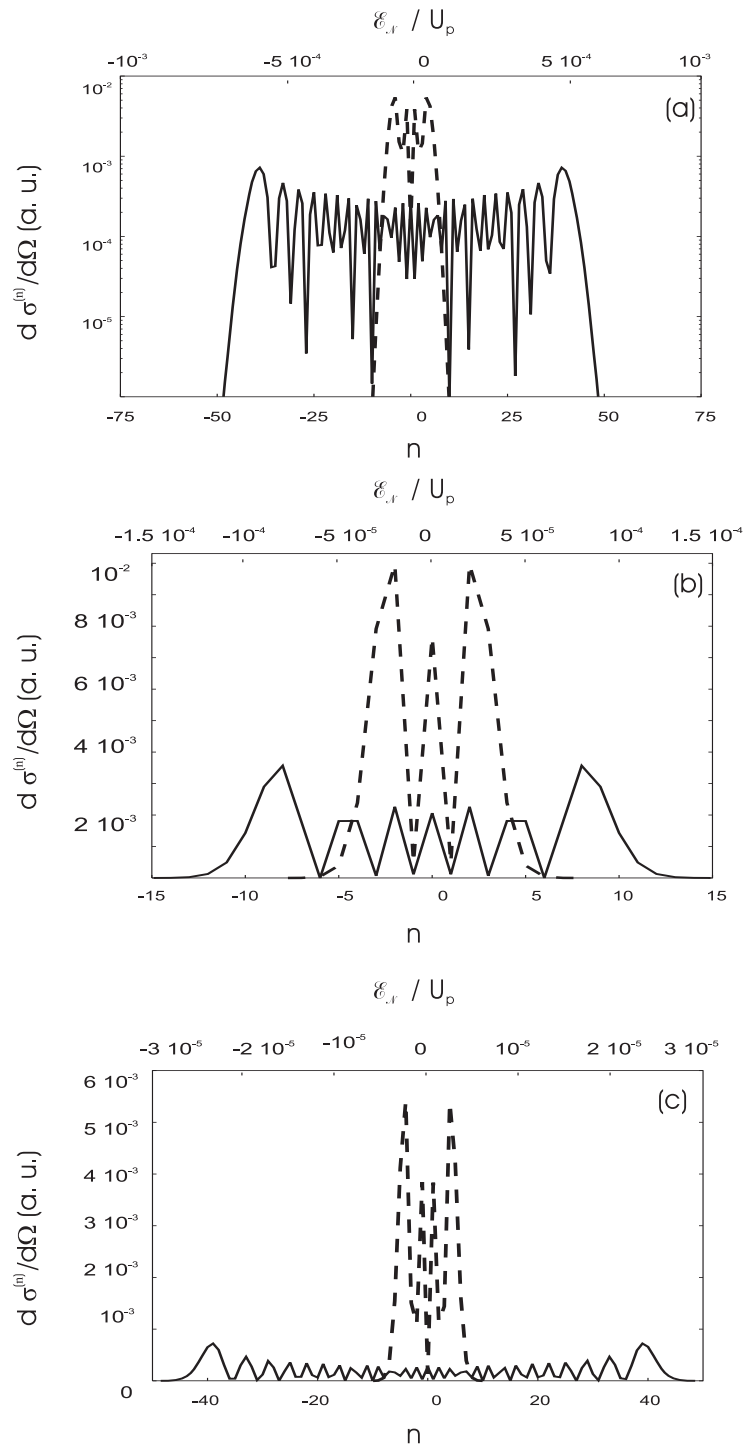


Fig. 4. The envelopes of partial differential cross-sections $d\sigma^{(n)}/d\Omega$ as a function of the number of emitted or absorbed photons, for the circularly polarized Ti-sapphire laser, in logarithmic scale. The dashed line corresponds to initial electron momentum antiparallel to the laser propagation direction, and the solid line gives the nonrelativistic result. The case (a) corresponds to $\xi=0.6$ for the deflection angle $\theta=0.6$ mrad, (b) $\xi=1$ for the deflection angle $\theta=60$ μ rad, and (c) $\xi=1.5$ for the deflection angle $\theta=6$ μ rad (the initial energy of the electron is taken to be $4U_p$).

As seen from Fig. 6, the main peaks in the angular distributions of photoelectrons in relativistic case are shifted towards the direction of the wave propagation, in contrast to nonrelativistic case when the angular distribution of electrons in the SB spectrum are typically aligned along the electric field of e.m. wave. The latter is also evident for the differential cross-section summed over photon numbers:

$$\frac{d\sigma}{d\Omega} = \sum_{n=-n_0}^{\infty} \frac{d\sigma^{(n)}}{d\Omega}, \quad (10)$$

which is displayed in Fig. 7 (a) for various laser intensities. In Fig. 7 (b) the summed AE differential cross-sections $d\sigma_{AE}/d\Omega$ (9) are represented. In (10) n_0 is the maximum number of emitted photons:

$$n_0 = \frac{\Pi_0 - m_*}{\omega}, \quad (11)$$

and

$$m_* = \sqrt{\Pi_0^2 - \vec{\Pi}^2} = \sqrt{m^2 + \frac{e\bar{A}_0^2}{2}} \quad (12)$$

is the "effective mass" of the relativistic electron in the e.m. wave field.

In the case of linearly polarized e.m. wave the function $d\sigma/d\Omega$ have many peaks, in contrast to the case of the circularly polarized e.m. wave [11] where differential cross-section has one peak.

To show the dependence of SB process upon laser intensity in Fig. 8, the envelopes of summed AE differential cross-sections are plotted for various deflection angles as a function of the intensity parameter ξ .

The electron initial momentum is parallel to the e.m. wave propagation direction. The dependence is essentially nonlinear in contrast to the perturbation theory, where the n -photon SB cross-sections $\approx \xi^{2n}$.

In Fig. 9 the envelopes of integrated AE partial cross-sections $\sigma_{AE}^{(n)}$ for various laser intensities as a function of the photon number are plotted for various laser intensities. Negative values correspond to net emission, while positive values correspond to net absorption. From Fig. 9 we see that AE partial cross-section is an oscillating function.

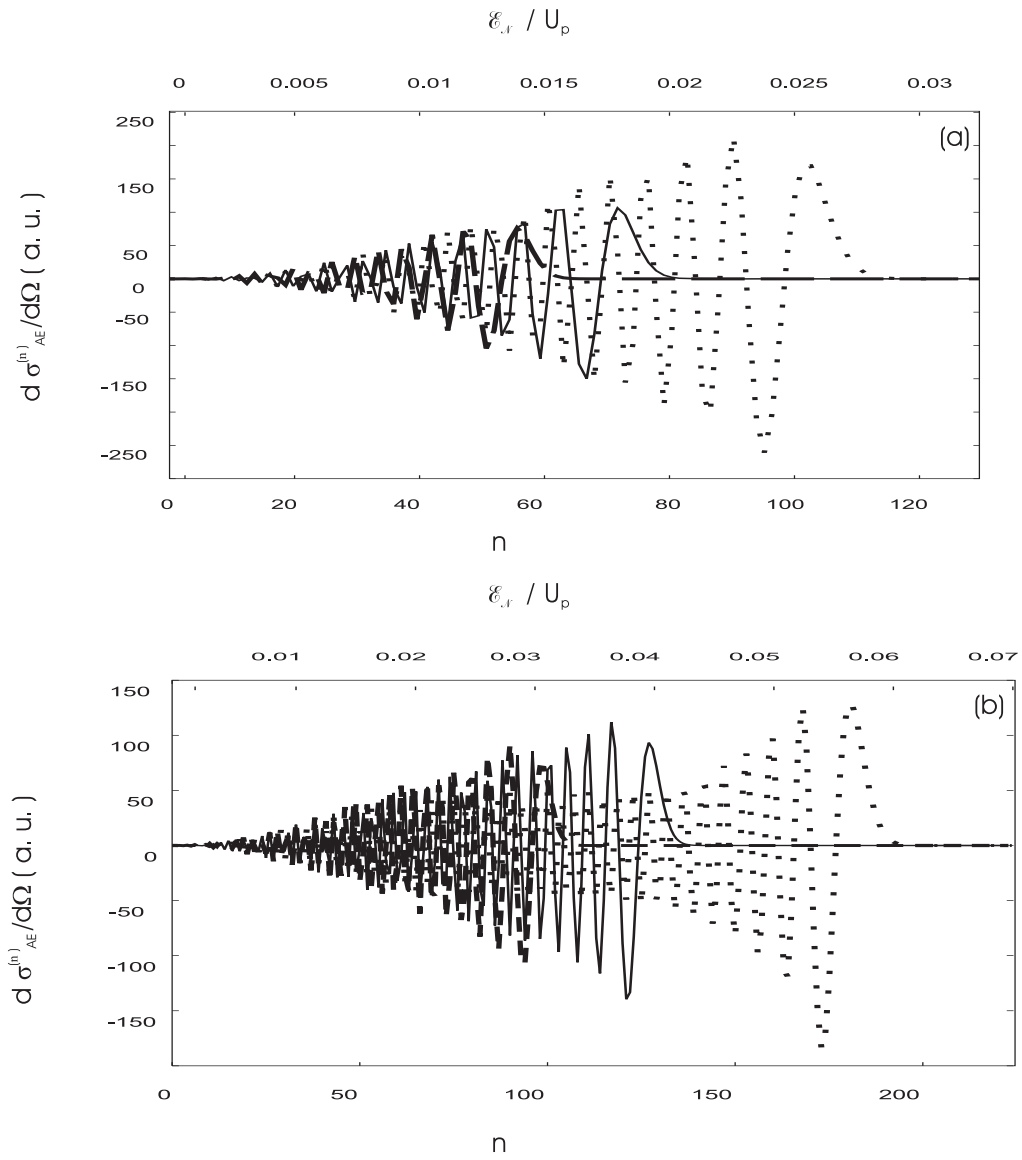


Fig. 5. The envelopes of partial absorption/emission differential cross-sections are shown in the cases of the large deflection angles: (a) $\theta=4.6$ mrad, and (b) $\theta=10$ mrad. The relativistic parameter of intensity $\xi=0.2$ ($\omega=0.058$ a.u.). The initial energy of an electron is taken to be 2.7 keV.

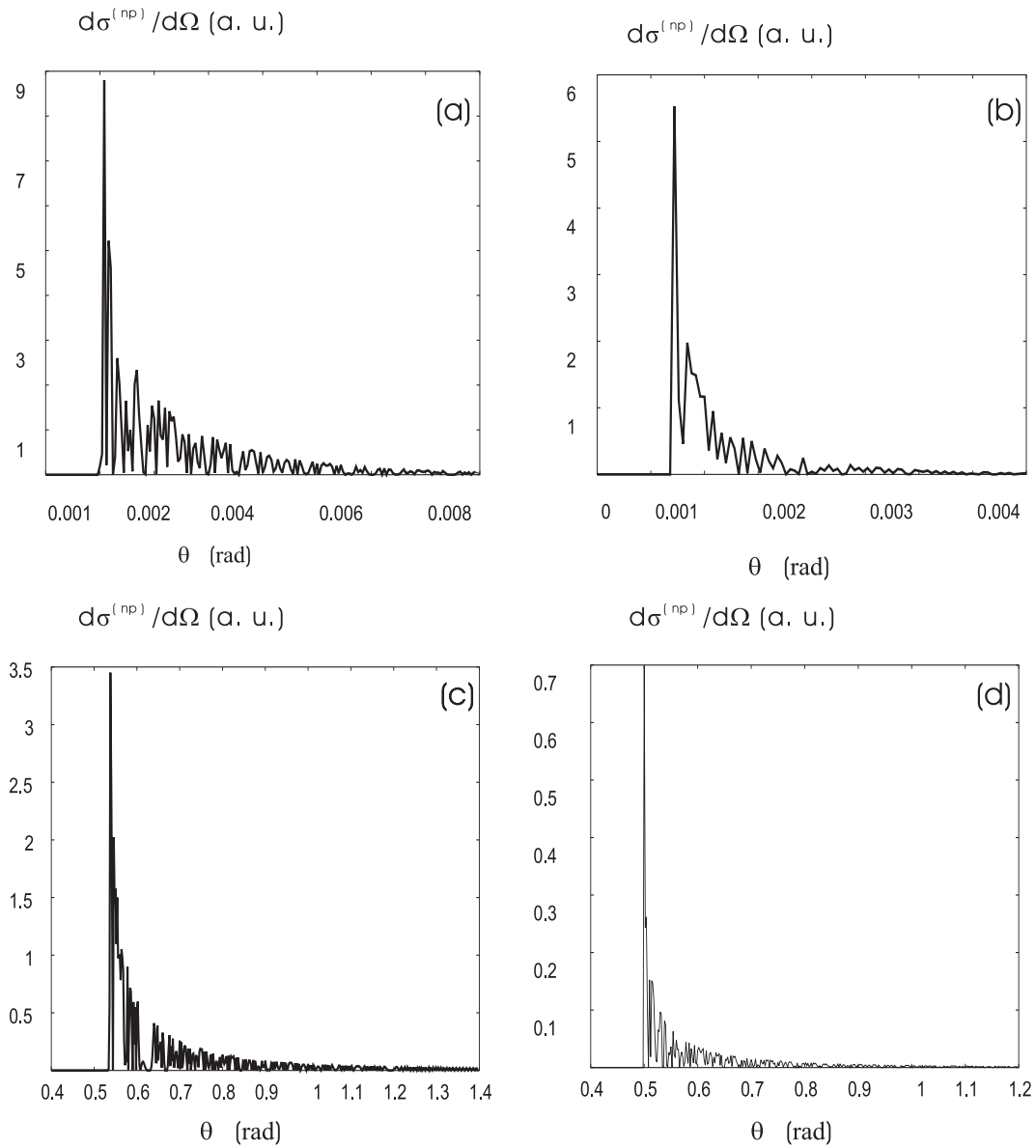


Fig. 6. The partial cross-sections $d\sigma^{(n)}/d\Omega$ as a function of the polar angle θ (with respect to the wave propagation direction) for the fixed value of number n_p of photons absorbed in the SB process. The electron moves in the laser propagation direction \vec{k} . The figures (a) and (b) correspond to linear polarization of the e.m. wave and $n_p=2U_p/\omega$. The figures (c) and (d) correspond to circular polarization of the e.m. wave, and $n_p=4U_p/\omega$. The intensity parameter $\xi=0.6$ for (a) and (c), while for (b) and (d) $\xi=1$.

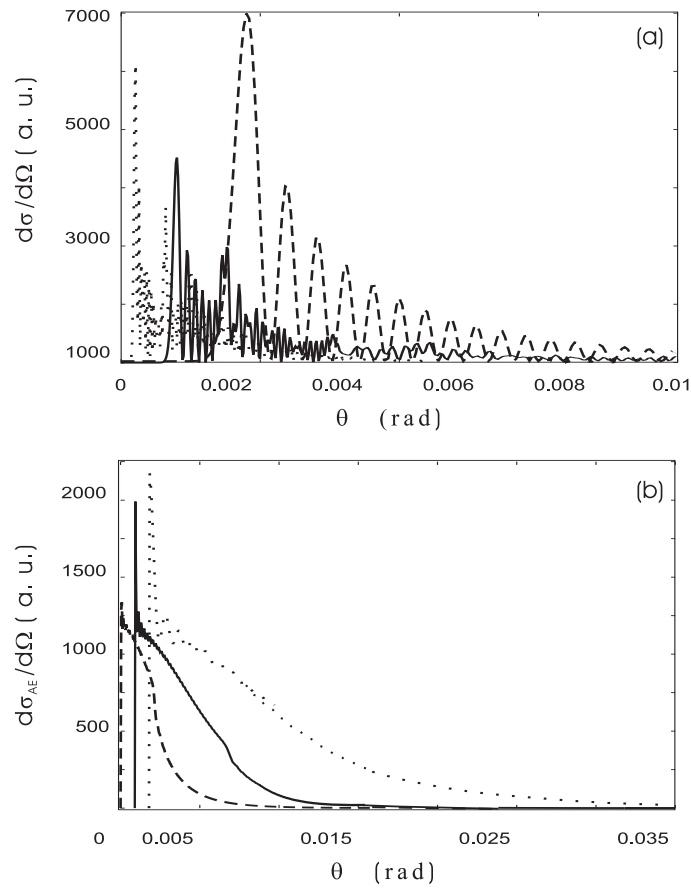


Fig. 7. The angular dependence of SB process for various laser intensities at linear polarization of e.m. wave. Part (a) displays summed differential cross-section $d\sigma/d\Omega$ as a function of the deflection angle θ , and (b) displays the absorption/emission differential cross-section $d\sigma_{AE}/d\Omega$, for the intensities of the laser field: $\xi=0.1$ (dashed line), $\xi=0.2$ (solid line), and $\xi=0.3$ (dotted line). The initial energy of an electron is taken to be 2.7 keV and initial electron momentum is parallel to the laser propagation direction \vec{k} .

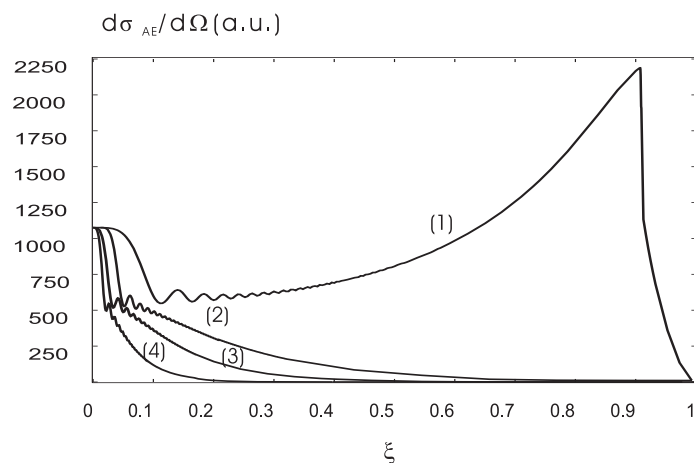


Fig. 8. The summed differential AE cross-sections $d\sigma_{AE}/d\Omega$ for linear polarization of e.m. wave are plotted as a function of relativistic parameter of intensity ξ in the range $0 < \xi < 1$ for deflection angles: $\theta=0.5$ mrad (line 1), $\theta=4$ mrad (line 2), $\theta=8$ mrad (line 3), and $\theta=16$ mrad (line 4). The initial electron momentum is parallel to the laser propagation direction \vec{k} . The initial energy of an electron is taken to be 2.7 keV.

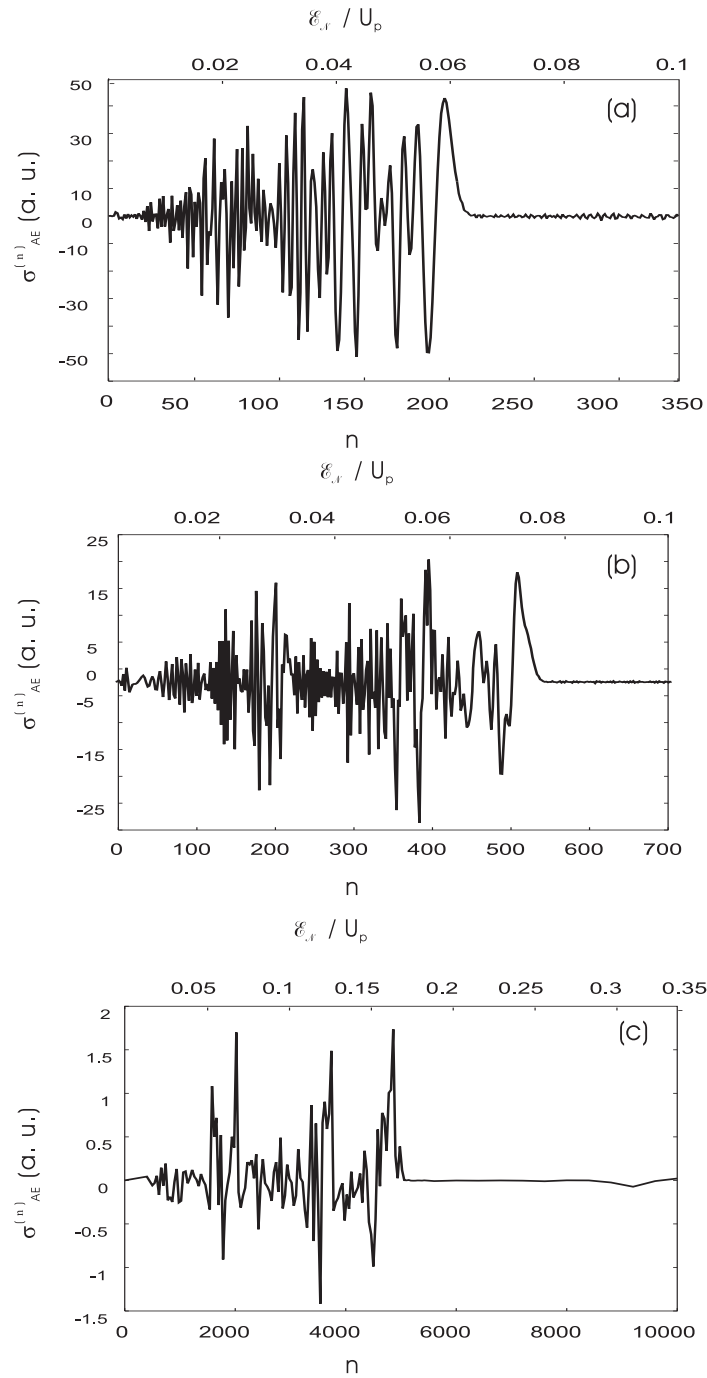


Fig. 9. The envelopes of integrated absorption/emission partial cross-sections $\sigma_{AE}^{(n)}$ for the linear polarization of e.m. wave as a function of the number of photons: a) $\xi=0.2$, b) $\xi=0.3$, and c) $\xi=0.6$. The initial electron momentum is parallel to the laser propagation direction \vec{k} .

In conclusion, we have presented SB process in the field of superstrong e.m. radiation of linear polarization. The scattering potential has been described in the Born approximation. The numerical analysis shows that SB in strong laser fields is essentially nonlinear, the multiphoton absorption/emission processes and relativistic effects play significant role already for moderate laser intensities (already at $\xi \ll 1$) in contrast, for example, to nonlinear Compton scattering [17],

where multiphoton processes become essential for $\xi \approx 1$ and the cutoff number of absorbed photons $\approx \xi^3$. SB and AE cross-sections have a tendency to fall with the increase in the wave intensity.

Acknowledgments

I would like to thank Prof. H.K. Avetissian and G.F. Mkrtchian for the recommendations and valuable discussions during the work on the present paper. This work was supported by International Science and Technology Center Project No. A-1307.

References

1. H. K. Avetissian, *Relativistic Nonlinear Electrodynamics*, Springer, New York, 2006.
2. F. V. Bunkin and M. V. Fedorov, *Sov. Phys. JETP* **22**, 844 (1966).
3. M. M. Denisov, M. V. Fedorov, *Sov. Phys. JETP* **26**, 779 (1968).
4. C. Szymanovsky, V. Veniard, R. Tajeb, A. Maquet, and C. H. Keitel, *Phys. Rev. A* **56**, 3846 (1997).
5. C. Szymanovsky, A. Maquet, *Opt. Express* **2**, 262 (1998).
6. L. S. Brown and R. L. Goble, *Phys. Rev. A* **173**, 1505 (1968); N. M. Kroll and K. M. Watson, *Phys. Rev. A* **8**, 804 (1973); J. Kaminski, *J. Phys. A* **18**, 3365 (1985).
7. H. K. Avetissian, A. K. Avetissian, K. Z. Hatsagortsian, and S. V. Movsissian, *J. Phys. B* **25**, 3201 (1992).
8. H. K. Avetissian, A. K. Avetissian, H. A. Jivanian, and S. V. Movsissian, *J. Phys. B* **25**, 3217 (1992).
9. H. K. Avetissian and S. V. Movsissian, *Phys. Rev. A* **54**, 3036 (1996).
10. H. K. Avetissian, K. Z. Hatsagortsian, A. G. Markossian, and S. V. Movsissian, *Phys. Rev. A* **59**, 549 (1999).
11. T. R. Hovhannisyan, A. G. Markossian, and G. F. Mkrtchian, *Eur. Phys. J. D* **20**, 17 (2002).
12. H. K. Avetissian, A. G. Markossian, and G. F. Mkrtchian, *Phys. Rev. A* **64**, 053404 (2001).
13. G. A. Mourou, T. Tajima, and S. V. Bilanov, *Rev. Mod. Phys.* **78**, 309 (2006); F. Krausz and M. Ivanov, *Rev. Mod. Phys.* **81**, 163 (2009).
14. H.K. Avetissian, A.G. Markossian, *Int. Conference of Photonic, Electronic, Atomic Collisions (ICPEAC'09)*, Kalamazoo, Michigan, July 22 -- 28, Poster sessions at **We040** (2009).
15. H. K. Avetissian, A. G. Markossian, *Phys. Rev. A* **76**, 053407 (2007).
16. T. Brabec and F. Krausz, *Rev. Mod. Phys.* **72**, 545 (2000).
17. V. I. Ritus, *Trudi Fiz. Inst. Akad. Nauk* **111**, 141 (1979).